Tribology and Materials
Vol. 2, No. 4, 2023, pp. 181-188
ISSN 2812-9717
https://doi.org/10.46793/tribomat.2023.019

Numeric simulation of steel twin disc system under rolling-sliding contact

Awet Gebretsadkan BRHANE [1,*], **Samuel Tesfaye MEKONONE** [2]

[1] Faculty of Mechanical and Industrial Engineering, Aksum University, Aksum, Ethiopia
[2] Institute of Technology, University of Gondar, Gondar, Ethiopia
*Corresponding author: awet1210@gmail.com

Keywords
twin disc system
friction
compressive load
contour region
finite element method

History
Received: 19-10-2023
Revised: 15-11-2023
Accepted: 20-11-2023

Abstract

Various mechanical parts come into high-load rolling and sliding contact at the contact surface. Even with technological advancements, mechanical failures still occur. Rolling-sliding mechanical contact issues are the primary cause of over 90 % of surface and subsurface metallic failures and they are only becoming worse. Using discretised continuum 2D finite element methods (FEM), this research investigates the parametric contact effect of a steel twin disc system subjected to rolling-sliding contact at varied surface friction and comprehensive load condition. The equivalent von Mises stress distribution, contact pressure distribution and shift position of maximum subsurface stress on the contour region are all influenced by changes in compressive load and coefficient of friction, according to a numerical surface-to-surface contact simulation performed with Abaqus at mean Hertzian pressure. The maximal equivalent stress, for a given load, reaches a peak in the subsurface and moves farther away from the surface when the coefficient of friction decreases and comes close to the contact surface when the coefficient of friction increases. Consistency is shown by the analytical and numerical results.

1. Introduction

Solid mechanics and tribology are fundamental disciplines of engineering that are indispensable for the manufacturing of safe and energy-saving designs. They are used in the majority of technical applications, such as electrical contacts, machining, cold forming, gearboxes, brakes, tires, bush and ball bearings, combustion engines, hinges, gaskets, castings and wheel-rail contacts. Their complex nature has prompted research into these and other applications [1-3]. Mechanical components undergo rolling-sliding contact subjected to high contact loads at the surface. Approximately 90 % of all metallic fatigue damage failures have been recorded due to mechanical causes. Many surface and subsurface rolling contact fatigue (RCF) failures are estimated to comprise in the United States and European rail systems exceeds many millions of dollars annually [4,5]. Comprehensive studies on the wheel-rail interface (approximated with cylindrical contact) have been conducted in the last decades, flourishing the horizon of different contact mechanics, wear and a phenomenon known as rolling-sliding contact fatigue which cause various engineered structures that come into contact with metallic surfaces to fail.

A two-dimensional numerical simulation of contact between a rigid flat surface and an elastic cylinder on the subsurface stress field of Hertzian contact under pure sliding conditions for different speeds and coefficients of friction is studied [6] and the 2D equivalent contact model together with Hertzian contact theory determines the influence of different parameters on the stress distribution of contact area [7]. The Hertz theory, the American Gear Manufacturers Association (AGMA) standard and the finite element method (FEM) have all been used to evaluate and validate the contact stress of spur gears with and without friction. The results show good agreement with minimum deviation [8,9]. In order to calculate stress caused by frictional heating on two-dimensional cylindrical plate rolling contact, theoretical and computational analysis of the mechanical and thermal wheel-rail frictional interaction was conducted using the finite element code Abaqus [10,11].

The influence of different parameters has been numerically studied with the model of cylindrical contact under rolling-sliding fatigue behaviour [12]. Hertz stress calculator software and finite element analysis address the stress issue at the contact surface showing that the finite element analysis (FEA) results are acceptable within 10 % error due to the approximation made as two half cylinders [13,14]. A finite element method has been developed and validated with an approach based on the Hertz theory for the determination of contact variables [15]. Two contact models based on the half-space assumption are compared and calculated using four different methods for modelling the wheel-rail rolling contact, and the results agree well with the finite element method (FEM) results [16]. Another paper tackles the phenomenon of unstable movement at the adhesive contact zone and shows consistency of the results using analytical, numerical and experimental analysis of adhesive contacts subjected to tangential motion [17]. Modelling of metal-to-metal sliding contact wear is still ongoing research using Abaqus to extract contact pressure at the contact surface [18].

Numerical methods are the most common techniques that can be used for different materials to determine contact parametric effects. This research work aims to determine the effect of compressive load and friction on contact stress and contact pressure by developing a two-dimensional Hertzian contact with a finite element method for a steel twin disk system under rolling-sliding contact.

2. Materials property and studied geometry

The material properties for the steel twin disc system (counter-face disc that is used to apply a compressive contact load and slave disk that is subjected to a contact load) are obtained for the analyses of Hertzian contact pressures and stress. The research was made using the dimensions and properties of two contacting materials where the geometry and material properties are obtained from the literature [19,20] as reported in Table 1.

Table 1. Material property and geometry of twin discs

Property	Disc 1 (master)	Disc 2 (slave)
Yield strength σ_y, MPa	856	720
Modulus of elasticity E, GPa	210	155
Poisson's ratio v	0.30	0.27
Rotational speed n, rpm	360	400
Contact length L, mm	1	1
Radius of curvature R, mm	20	20

2.1 Equivalent Hertzian contact modelling

The contact formulation of computational simulation for non-conformal contacting mechanical elements makes it advantageous to use a substitute model of two contacting cylinders, i.e. use of a cylinder on the half-space model. The interface of the rotating master (bearing steel) and slave disc (sintered steel), which are fixed at their centres, is subjected to distributed Hertzian pressure due to a normal contact force, that affects stress and contact pressure. Then, the problem can be reduced from a rolling-sliding contact to a quasi-static sliding contact [21-23]. The reduced equivalent contact model utilises the simplified equivalent Hertzian contact model and plain strain condition as described in Figure 1.

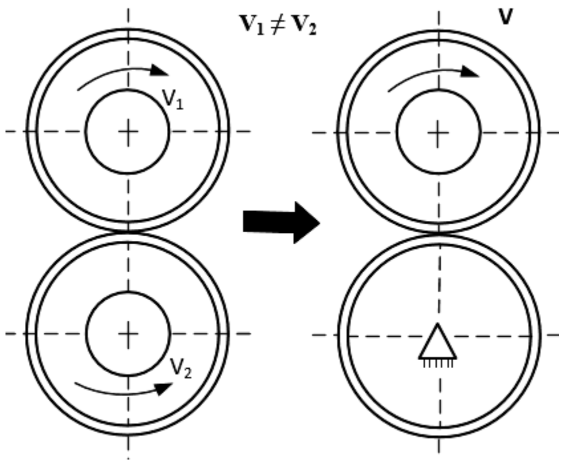

Figure 1. Equivalent contact model of twin disc rolling-sliding elements

2.2 Theoretical Hertzian stress analysis

According to the Hertzian theory, contact deformation under an external load has a relationship with the outlines of the contact surfaces and the external load. This means that the contact deformation is determined by two factors: the geometry of the contact surfaces and the external load. In this study, based on the given contact geometry of the master and slave disc, a normal force of 475 N was used to simulate the maximum contact pressure of approximately 1200 MPa between the cylindrical disc interface according to the Hertzian theory. The tangential force between the disc specimens was approximately 135 N. According to the Hertzian contact theory, the pressure distribution p is parabolic in shape in the contact width $2b$, and pressure becomes maximum $p_{\max}$ at the middle of the contact zone. The principal stress distribution of a cylindrical elastic contact is given by [24] and can be understood clearly by the given equations from the 2D Hertzian stress distribution theory.

$$\sigma_x = \frac{p_{\max}}{b}\left\{m\left(1+\frac{z^2+n^2}{m^2+n^2}\right)-2z\right\}, \quad (1)$$

$$\sigma_z = \frac{p_{\max}}{b}m\left(1-\frac{z^2+n^2}{m^2+n^2}\right), \quad (2)$$

$$\sigma_y = v\,(\sigma_x+\sigma_z). \quad (3)$$

For a line contact between two cylinders, the stress distribution at any space directions (x, z) based on the variable signs of m and n (arbitrary positions) is given by [24] as follows:

$$m^2 = \frac{1}{2}\left[\left\{(b^2-x^2+z^2)^2+4x^2z^2\right\}^{1/2} + \right.$$
$$\left. +(b^2-x^2+z^2)\right], \quad (4)$$

$$n^2 = \frac{1}{2}\left[\left\{(b^2-x^2+z^2)^2+4x^2z^2\right\}^{1/2} - \right.$$
$$\left. -(b^2-x^2+z^2)\right]. \quad (5)$$

The equivalent Hertzian mechanical stress is given by equation [25]:

$$\sigma_{\text{eq.}} = \frac{1}{2}\left[(\sigma_z-\sigma_x)^2+(\sigma_y-\sigma_x)^2 + \right.$$
$$\left. +(\sigma_z-\sigma_y)^2\right]^{1/2}. \quad (6)$$

Maximum shear stress is determined by the principal stresses [25]:

$$\tau_{\max} = \begin{cases} \tau_{xz} = \dfrac{\sigma_z-\sigma_x}{2} & \text{for } \dfrac{z}{b} < 0.463 \\ \tau_{yz} = \dfrac{\sigma_z-\sigma_y}{2} & \text{for } \dfrac{z}{b} \geq 0.463 \end{cases}. \quad (7)$$

When the stress components shown in Equations (1) to (3) are plotted below the surface as a function of maximum contact pressure and based on Poisson's ratio of 0.3, the maximum shear stress is either τ_{xz} or τ_{yz} based on the value of z/b at which both stresses intersect. For the specific input parameters, the maximum shear stress $\tau_{\max}$ is equal to τ_{xz} if $z/b < 0.463$, whereas equals τ_{yz} if $z/b \geq 0.463$, and its maximum value is 0.30 $p_{\max}$ [25].

The mean Hertzian pressure p_o applied to the cylindrical contact surface is determined using the relation given by [19,26], as follows:

$$p_o = 0.78\,p_{\max}, \quad (8)$$

where the maximum pressure $p_{\max}$ is given by Equation (9):

$$p_{\max} = \frac{2F}{\pi bL}, \quad (9)$$

where L is contact length and F is applied load.

Contact half-width b is related to the reduced modulus of elasticity E_c, equivalent radius of curvature R_c and applied load F, and is determined using Equation (10).

$$b = \sqrt{\frac{4R_c F}{\pi L E_c}}, \quad (10)$$

Reduced modulus of elasticity E_c and equivalent radius of curvature R_c are evaluated using Equation (11) and (12), respectively.

$$\frac{1}{E_c} = \frac{1-v_1^2}{E_1}+\frac{1-v_2^2}{E_2}, \quad (11)$$

$$\frac{1}{R_c} = \frac{1}{R_1}+\frac{1}{R_2}. \quad (12)$$

3. Numerical simulation procedure

3.1 Numerical model of non-conformal disc contact

A commercial finite element analysis package (Abaqus/Standard) is available to study the contact situation with various contact algorithms between two surfaces. The master-slave contact interaction (disc 1 to disc 2), in which the slave surface follows the master surface motion and experiences large relative motion, is used to simulate the two-dimensional surface and subsurface stresses. Finite element analysis simulations are performed to validate the theoretical models described above. A considerable number of attempts have been made to develop, model and simulate a twin disc rolling-sliding contact interface, as shown in Figure 2, through a two-dimensional linear elastic, 4-node (bilinear), plane strain quadrilateral, reduced integration element (CPE4R).

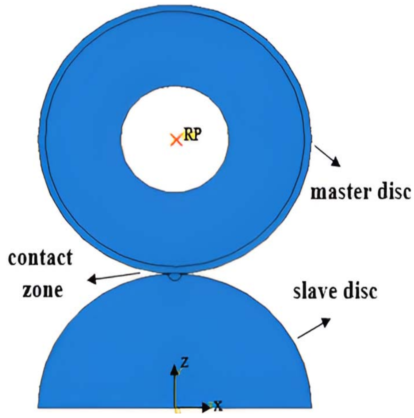

Figure 2. Numerical model of disc contact

Figure 3 shows the computational mesh used in the finite element method (FEM), in which only part of the cylinder is considered. The mesh size of 0.02 × 0.02 mm was considered at the contact interface and decreased gradually from the contact region for all models. The weaknesses of the bearing components, such as exceeding the allowable stress, undesirable deformation and stress distribution, could be calculated and optimised using quasi-static Abaqus software.

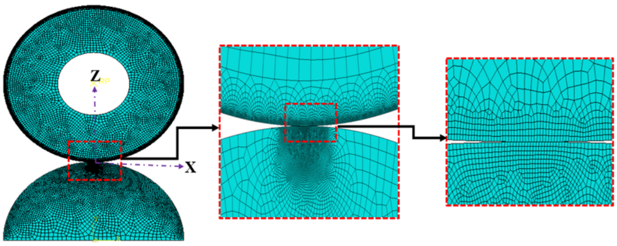

Figure 3. Mesh formulation at the contact surface

The disc boundary conditions are specified on the reference point associated with its geometry. The master disc (disc 1) is constrained from moving in the *z*-direction by the use of displacement boundary conditions set to zero. Concentrated nodal forces are applied to the displacement degrees of freedom, loaded in the *z*-direction at the centre of the master disc. Centre node movements in the *x*- and *z*-direction are suppressed, while the rotations around the *y*-axis are free. The slave disc is fixed at the bottom in all directions to simulate the actual movement of the disc as shown in Figure 2.

3.2 Convergence analysis

The solids bodies involved in the contact problem must be discretised into a finite element mesh and different solutions can be adopted. The mesh size at the contact interface (mesh refinement) should be fine with dense mesh to capture the relaxed stress state near the contact between the master and slave disc surface. Mesh convergence was performed to find a mesh size that produces correct results. Modelling with mesh refinement was continued until an appropriate convergence of the stress state was achieved without using too many elements, which would increase calculation time and computational power.

Different solutions can be adopted while meshing a master-slave disc for equivalent stress. According to the mesh convergence study results shown in Table 2, an acceptable element size in the refined contact zone was determined to be at least less than 0.02 mm.

4. Results and discussion

Shear and normal forces are typically transmitted across the interface of surfaces that are in contact. The stresses at the bodies' interface are typically used to describe this relationship between the contacting bodies. The equivalent mechanical von Mises stress and contact pressure on the contact surface bodies can be predicted using an analytical solution based on the Hertz contact stress theory. Finite element analysis software package Abacus has used finite elements to analyse the effects of friction and applied compressive load on von Mises stress, pressure distribution and contour region.

4.1 Effect of comprehensive contact load

The contact surface between the discs is used to simulate the equivalent mechanical von Mises stress along the depth with various compressive contact forces. Figure 4 illustrates this in general, i.e. at the contact surface, the equivalent mechanical von Mises stress and contact width increase with increasing load and vice versa along the contact width.

Table 2. Mesh convergence analysis

Mesh iteration number	Local mesh element size, mm	Number of elements	Numerical equivalent stress, MPa	Hertzian equivalent stress, MPa	Processing time, s
1	1	1362	240.65	690	337
2	0.5	4573	356.43	690	1247.2
3	0.1	10,073	672.60	690	2715.7
4	0.05	21,894	683.62	690	5420
5	0.02	57,652	688.87	690	19,680

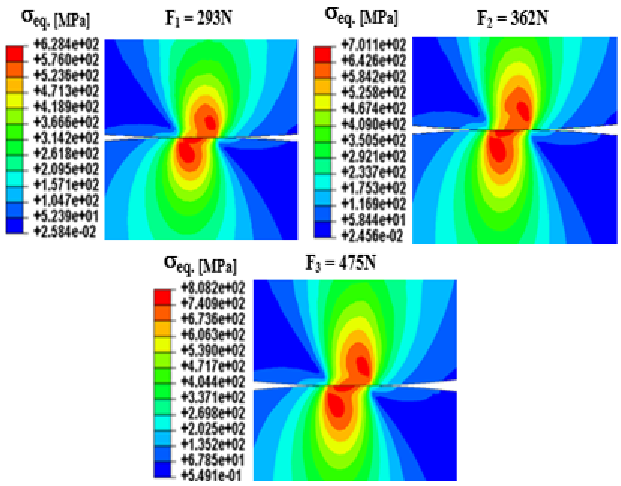

Figure 4. The effect of load on equivalent von Mises mechanical stress

The contact pressure and the contact width at different contact forces are simulated. Maximum pressure and contact width increase with contact load, as represented in Figure 5. The contact half-width b and maximum pressure p_{max} at 475 N are 0.5 mm and 1210 MPa, respectively.

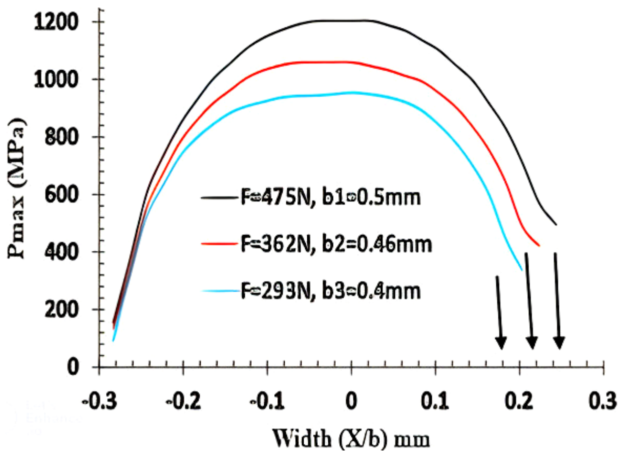

Figure 5. The effect of load on contact pressure along the normalised width (x/b) of contact

4.2 Effect of contact surface friction

Friction generally modifies the Hertzian stress distribution, which is amenable to numerical analysis. The position of maximum stress under the contact surface depends on friction as Figure 6 illustrates. When the coefficient of friction μ decreases, the equivalent von Mises stress decreases and reaches a peak far from the surface at the depth z, as shown in Figure 6. Conversely, when the coefficient of friction increases, the maximum equivalent von Mises stress increases and reaches its maximum at the contact surface (z = 0).

The equivalent mechanical maximum von Mises stress occurs at the contact surface when the coefficient of friction reaches a maximum of 0.3, and as friction decreases to zero, the maximum stress occurs somewhere far from the contact (in the subsurface), specifically at the depth of 157 μm (z = 0.63b), as illustrated in Figure 7.

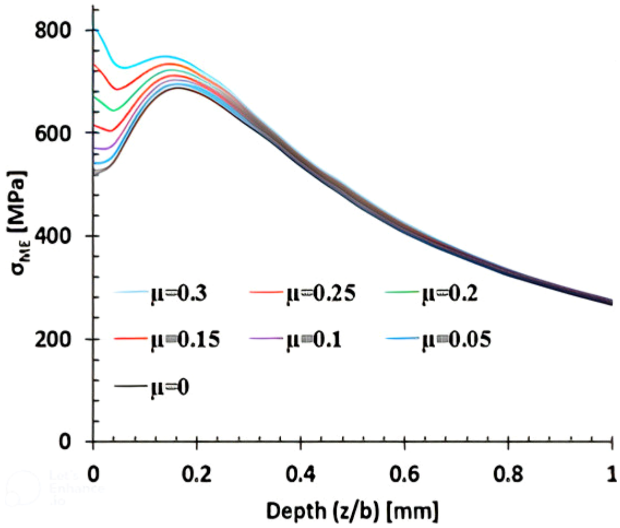

Figure 6. The impact of the coefficient of friction along normalised depth (z/b) on mechanical von Mises stress

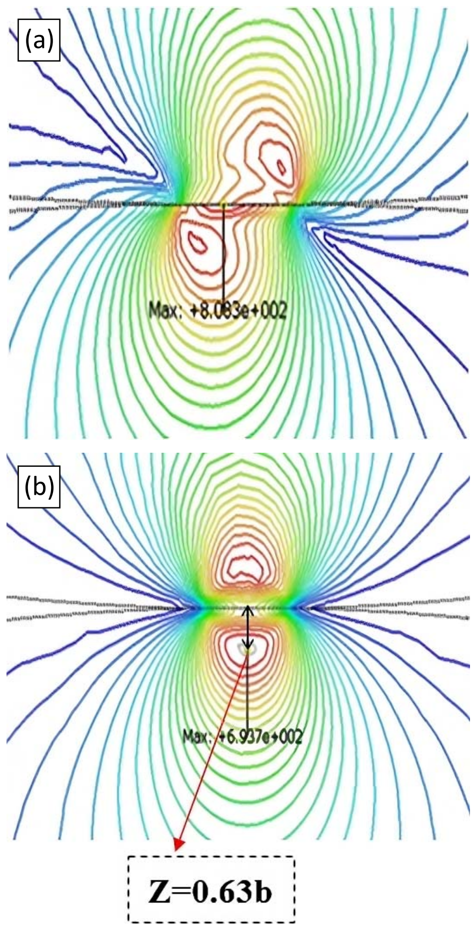

Figure 7. Maximum and minimum contour region (profile) of Hertzian equivalent stress at F= 475 N and: (a) μ = 0.3 and (b) μ = 0

At the maximum coefficient of friction, the contact pressure at the end of the contact (the outlet) is comparatively greater than the smallest contact pressure at the starting point of the contact (the inlet), and vice versa at the lowest coefficient of friction. This demonstrates how increasing the coefficient of friction causes the contact pressure to increase at the end of the contact and decrease at the beginning of the contact. The simulation result also verifies that the coefficient of friction has no significant effect on the contact pressure except, of course, a little influence at the start and end of the contact, as shown in Figure 8.

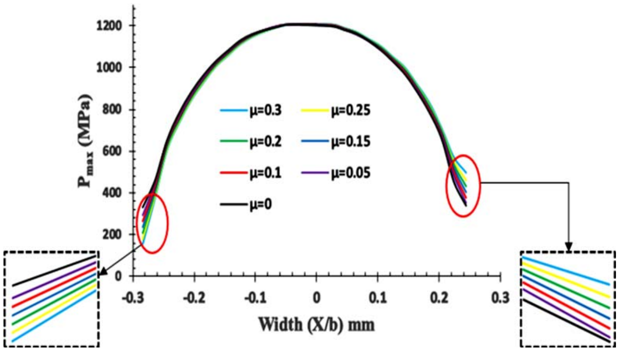

Figure 8. The effect of friction on contact pressure along the normalised width of contact

The developed contact model of two elastic bodies was verified through a comparison of the analytical solutions and numerical results, demonstrating consistency with less than 1 % error, as shown in Table 3. The stress value obtained from the finite element method (FEM) is less than that of the Hertz contact stress. Overall, the results show a strong correlation with one another and little variation. Table 3 illustrates how the number, type and distribution of meshing elements, as well as the mesh refining procedure, affect the difference between theory and finite element analysis (FEA). Acceptable accuracy, however, demands a respectable computation time, load applied step and contact constraints.

Table 3. Comparison of analytical and numerical results at F = 475 N and μ = 0

	von Mises stress $\sigma_{eq.}$	Mean contact pressure p_o
Numerical result, MPa	687.5	941.64
Analytical result, MPa	690	950
Error, %	0.34	0.88

4.3 The effect of contour deviation on the distribution of the subsurface stress profile

Significant changes are observed for the distribution of subsurface stress in contact elements and in deviation of the contact contour region profile, as depicted in Figure 7. The region of maximum stress appears to be shifted in the direction of sliding for coefficients of friction greater than 0.15, as illustrated in Figure 9. The shift increases as the coefficient of friction increases, so the shift of the contour contact region is minimal when the coefficient of friction is the lowest, showing that the stress distribution between the contact elements is perfectly symmetrical around the contact region area.

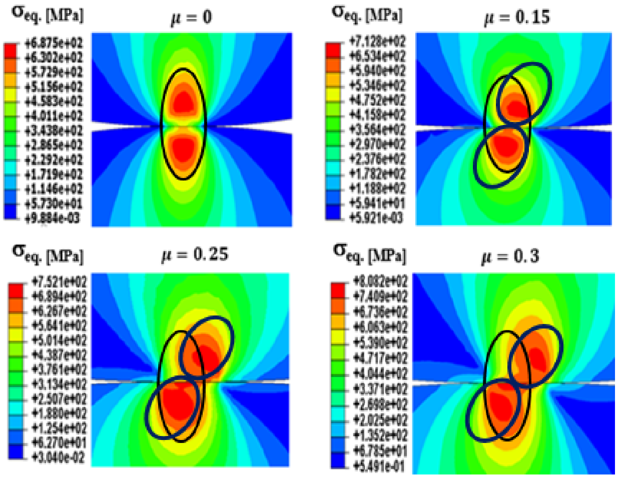

Figure 9. Contour deviation of Hertzian equivalent stress at F = 475 N and various values of μ

5. Conclusion

Due to the influence of contact forces and coefficient of friction, the 2D linear behaviour of surface-to-surface rolling-sliding, non-conformal elastic body contact formulation based on Hertzian elliptical contact theory is examined for the maximum stress distribution at every position of the x-z plane. Additionally, the analytical approach is used for this, while the finite element method (Abacus) is used for the related numerical analysis.

The von Mises stress and contact width are influenced by load, i.e. when load increases, the stress and contact width also increase. Friction has an impact on the Hertzian depth stress distribution, i.e. when friction decreases, stress decreases and extends below the surface and vice versa. Friction generally has little effect at the inlet and outlet of contact, but it does have some effect on the position and profile (contour region) of stress. The analytical result provides confidence in estimating the mechanical contact behaviour and exhibits a very good correlation with the static numerical simulation result under various conditions.

References

[1] V.L. Popov, Contact Mechanics and Friction, Springer, Berlin, 2010, DOI: 10.1007/978-3-642-10803-7

[2] M. Marin, A temporally evolutionary equation in elasticity of micropolar bodies with voids, Scientific Bulletin, Series A: Applied Mathematics and Physics, Vol. 60, No. 3-4, 1998, pp. 3-12.

[3] S. Vlase, C. Năstac, M. Marin, M. Mihălcică, A method for the study of the vibration of mechanical bars systems with symmetries, Acta Technica Napocensis, Series: Applied Mathematics, Mechanics and Engineering, Vol. 60, No. 4, 2017, pp. 539-544.

[4] M. Ghodrati, M. Ahmadian, R. Mirzaeifar, Modeling of rolling contact fatigue in rails at the microstructural level, Wear, Vol. 406-407, 2018, pp. 205-217, DOI: 10.1016/j.wear.2018.04.016

[5] L. Xin, V.L. Markine, I.Y. Shevtsov, Numerical analysis of rolling contact fatigue crack initiation and fatigue life prediction of the railway crossing, in Proceedings of the 10th International Conference on Contact Mechanics – CM2015, 30.08-03.09.2015, Colorado Springs, USA.

[6] F. Ali, Numerical study on subsurface stress in Hertzian contacts under pure sliding conditions, Journal of Applied and Computational Mechanics, Vol. 6, No. Special, 2020, pp. 1098-1106, DOI: 10.22055/jacm.2019.31511.1882

[7] G. Fajdiga, Computational fatigue analysis of contacting mechanical elements, Tehnički vjesnik, Vol. 22, No. 1, 2015, pp. 169-175, DOI: 10.17559/TV-20140429122305

[8] M. Farhan, S. Karuppanan, S.S. Patil, Frictional contact stress analysis of spur gear by using finite element method, Applied Mechanics and Materials, Vol. 772, 2015, pp. 159-163, DOI: 10.4028/www.scientific.net/AMM.772.159

[9] S. Olguner, İ.H. Filiz, Contact and bending stress analysis of spur gear drives, in Proceedings of the 16th International Conference on Machine Design and Production, 30.06-03.07.2014, İzmir, Turkey, Paper 67.

[10] A. Draganis, F. Larsson, A. Ekberg, Finite element modelling of frictional thermomechanical rolling/sliding contact using an arbitrary Lagrangian-Eulerian formulation, Proceedings of the Institution of Mechanical Engineers, Part J: Journal of Engineering Tribology, Vol. 229, No. 7, 2015, pp. 870-880, DOI: 10.1177/1350650115572197

[11] W. Li, Z. Wen, X. Jin, L. Wu, Numerical analysis of rolling-sliding contact with the frictional heat in rail, Chinese Journal of Mechanical Engineering, Vol. 27, No. 1, 2014, pp. 41-49, DOI: 10.3901/CJME.2014.01.041

[12] J-F. Brunel, E. Charkaluk, P. Dufrénoy, F. Demilly, Rolling contact fatigue of railways wheels: Influence of steel grade and sliding conditions, Procedia Engineering, Vol. 2, No. 1, 2010, pp. 2161-2169, DOI: 10.1016/j.proeng.2010.03.232

[13] P. Purushothaman, P. Thankachan, Hertz contact stress analysis and validation using finite element analysis, International Journal for Research in Applied Science and Engineering Technology, Vol. 2, No. 11, 2014, pp. 531-538.

[14] S. Patil, S. Karuppanan, I. Atanasovska, A.A. Wahab, Frictional tooth contact analysis along line of action of a spur gear using finite element method, Procedia Materials Science, Vol. 5, 2014, pp. 1801-1809, DOI: 10.1016/j.mspro.2014.07.399

[15] I. Gonzalez-Perez, J.L. Iserte, A. Fuentes, Implementation of Hertz theory and validation of a finite element model for stress analysis of gear drives with localized bearing contact, Mechanism and Machine Theory, Vol. 46, No. 6, 2011, pp. 765-783, DOI: 10.1016/j.mechmachtheory.2011.01.014

[16] M. Wiest, E. Kassa, W. Daves, J.C.O. Nielsen, H. Ossberger, Assessment of methods for calculating contact pressure in wheel-rail/switch contact, Wear, Vol. 265, No. 9-10, 2008, pp. 1439-1445, DOI: 10.1016/j.wear.2008.02.039

[17] V.L. Popov, Q. Li, I.A. Lyashenko, R. Pohrt, Adhesion and friction in hard and soft contacts: Theory and experiment, Friction, Vol. 9, No. 6, 2021, pp. 1688-1706, DOI: 10.1007/s40544-020-0482-0

[18] M. Baby, K.R. Jayadevan, Finite element modelling of sliding contact wearin aluminium, in Proceedings of Third International Conference on Materials for the Future – ICMF 2013, 06-08.11.2013, Thrissur, India, pp. 70-77.

[19] S.T. Mekonone, W. Pahl, A. Molinari, Influence of the microstructure on the subsurface and surface damage during lubricated rolling-sliding wear of sintered and sinterhardened 1.5%Mo-2%Cu-0.6%C steel: Theoretical analysis and experimental investigation, Powder Metallurgy, Vol. 61, No. 3, 2018, pp. 187-196, DOI: 10.1080/00325899.2018.1446706

[20] S. Tesfaye Mekonone, I. Cristofolini, W. Pahl, A. Molinari, Surface hardening vs. surface embrittlement in carburizing of porous steels, Powder Metallurgy Progress, Vol. 18, No. 1, 2018, pp. 21-30, DOI: 10.1515/pmp-2018-0003

[21] E.S. Alley, Influence of Microstructure in Rolling Contact Fatigue of Bearing Steels with Inclusions, PhD thesis, College of Engineering, Georgia Institute of Technology, Atlanta, 2009.

[22] V. Hegadekatte, S. Kurzenhäuser, N. Huber, O. Kraft, A predictive modeling scheme for wear in

tribometers, Tribology International, Vol. 41, No. 11, 2008, pp. 1020-1031, DOI: 10.1016/j.triboint.2008.02.020

[23] R. Ismail, Running-in of Rolling-Sliding Contacts, PhD thesis, Faculty of Engineering Technology, University of Twente, Enschede, 2013, DOI: 10.3990/1.9789036518871

[24] K.L. Johnson, Contact Mechanics, Cambridge University Press, Cambridge, 1985, DOI: 10.1017/CBO9781139171731

[25] R.G. Budynas, J.K. Nisbett, Shigley's Mechanical Engineering Design, McGraw-Hill, New York, 2011.

[26] G. Straffelini, Friction and Wear, Springer, Cham, 2015, DOI: 10.1007/978-3-319-05894-8